

From DIS to proton-nucleus collisions in the Color Glass Condensate model

François Gelis⁽¹⁾ and Jamal Jalilian-Marian⁽²⁾

October 27, 2018

1. Service de Physique Théorique
Bât. 774, CEA/DSM/Saclay
91191, Gif-sur-Yvette Cedex, France
2. Physics Department
Brookhaven National Laboratory
Upton, NY 11973, USA

Abstract

We show that particle production in proton-nucleus (pA) collisions in the Color Glass Condensate model can be related to Deep Inelastic Scattering of leptons on protons/nuclei (DIS). The common building block is the quark antiquark (or gluon-gluon) dipole cross section which is present in both DIS and pA processes. This correspondence in a sense generalizes the standard leading twist approach to pA collisions based on collinear factorization and perturbative QCD, and allows one to express the pA cross sections in terms of a universal quantity (dipole cross section) which, in principle, can be measured in DIS or other processes. Therefore, using the parameterization of dipole cross section at HERA, one can calculate particle production cross sections in proton-nucleus collisions at high energies. Alternatively, one could use proton-nucleus experiments to further constrain models of the dipole cross-section. We show that the McLerran-Venugopalan model predicts enhancement of cross sections at large p_{\perp} (Cronin effect) and suppression of cross sections at low p_{\perp} . The cross over depends on rapidity and moves to higher p_{\perp} as one goes to more forward rapidities.

SPhT-T02/167

1 Introduction

High gluon density effects at high energy (small x) have been the subject of intense theoretical and experimental investigation [1, 2, 3, 4, 5, 6, 7, 8, 9, 10, 11, 12, 13, 14, 15, 16, 17, 18, 19, 20]. At small x , the number of gluons per unit area

and rapidity in the wave function of a high energy hadron or nucleus becomes large and the high energy hadron or nucleus can be described by a classical color field. Since most of the gluons in the wave function of a high energy hadron or nucleus are in a coherent state characterized by their typical momentum Q_s , a high energy hadron or nucleus is dubbed a Color Glass Condensate. An effective action and renormalization group approach has been developed which enables one to calculate cross sections in a high gluon density environment.

In [21, 22, 23, 24], for proton-nucleus collisions at high energies and in the forward rapidity region¹ we proposed describing the proton by the QCD parton model and the nucleus by the Color Glass Condensate model. One can then relate particle production in proton-nucleus collisions to the scattering of a quark or gluon from the Color Glass Condensate [21, 22, 23, 24]. Here we show that one can relate particle production in proton-nucleus collisions to Deep Inelastic Scattering of electrons (or more precisely, virtual photons) on protons and nuclei. This is due to the fact that the description of the target as a Color Glass Condensate is universal and independent of the process considered.

While the relation between particle production in proton-nucleus collisions and DIS structure functions has been known for a while in the case of dilepton² (virtual photon) production [25, 26] (and references therein), here we show that this relation is more general in our framework and holds for production of any particle (which has a known fragmentation function) in proton-nucleus collisions at high energy. This is crucial in view of the upcoming proton (deuteron)-nucleus experiments at RHIC. One would like to have predictions from QCD with as few model dependent assumptions about nuclear effects as possible.

In proton-proton collisions, standard calculations are based on collinear factorization theorems, proven at the leading twist level. The predictability of the theory is due to the fact that the building blocks (distribution or fragmentation functions) used in the cross section are universal (i.e. process independent) objects which can be measured in a given process and used to predict the outcome of other processes. It is well known that higher twist effects break collinear factorization and one has to resort to other methods. In proton-nucleus collisions, in order to take nuclear modifications such as shadowing and Cronin effect into account, one commonly modifies the parton distributions to include nuclear shadowing and introduces some model for Cronin effect. The parameters of the model are then constrained by fits to the existing data and used to make predictions for other processes or higher energies.

However, it is clear that this approach cannot be true in general since collinear factorization theorems break down due to higher twist (multiple scatterings) effects which become significant in scattering off nuclei. Therefore there is no guarantee that the parameters of such models are universal and process independent and these models have little predictive power. Here we show that one can generalize the standard leading twist expressions in such a way that all higher twist effects are included and the universality of the building blocks

¹By forward rapidity region we mean, roughly, any rapidity between proton rapidity and mid-rapidity.

²We would like to thank Y. Kovchegov for pointing this out to us.

(dipole cross sections) of the theory is preserved and the predictive power of the theory is restored.

2 Reminder: DIS and the dipole cross-section

2.1 DIS amplitude

We first start by a brief reminder of how the dipole cross-section appears in Deep Inelastic Scattering. This calculation will in fact be useful in order to compare with the very similar problem of dilepton (i.e. virtual photon) production in pA collisions. The nucleus is treated using the Color Glass Condensate model, i.e. as a set of classical and randomly distributed color sources that generate a classical field. There are three relevant diagrams for the DIS amplitude in this model, which are represented in figure 1. In this figure, the black dot

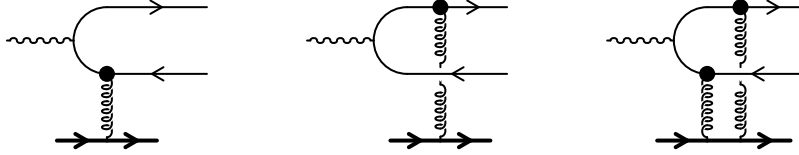


Figure 1: The relevant diagrams for $\gamma^* A \rightarrow q\bar{q}X$ in the Color Glass Condensate model. The black dots denote the eikonal interaction between the quark or antiquark with the classical color field.

denotes the eikonal all-orders interaction between a quark or antiquark with the classical field of the nucleus. More precisely, for a quark or antiquark line in which the incoming momentum is P and the outgoing momentum³ is Q , the (time-ordered) eikonal scattering amplitude reads

$$T_{\text{eik}}(Q, P) = 2\pi\delta(q^- - p^-)\gamma^- \text{sign}(p^-) \int d\mathbf{x}_\perp e^{i(\mathbf{q}_\perp - \mathbf{p}_\perp) \cdot \mathbf{x}_\perp} \left(U^{\text{sign}(p^-)}(\mathbf{x}_\perp) - 1 \right), \quad (1)$$

where we assume that the nucleus is moving close to the speed of light in the $+z$ direction. $U(\mathbf{x}_\perp)$ is a matrix living in the fundamental representation of $SU(N_c)$, given by

$$U(\mathbf{x}_\perp) \equiv \text{T exp} \left\{ -ig^2 \int_{-\infty}^{+\infty} dz^- \frac{1}{\nabla_\perp^2} \rho_a(z^-, \mathbf{z}_\perp) t^a \right\}, \quad (2)$$

with t^a in the fundamental representation, and where $\rho_a(z^-, \mathbf{z}_\perp)$ is the density of color sources in the nucleus. How to average over these sources is explained in [27, 23].

³We use the following notations throughout this paper: P denotes a 4-momentum, \mathbf{p} denotes its spatial part, \mathbf{p}_\perp its transverse components, and p^\pm its longitudinal components in light-cone variables.

We first compute the $\gamma^* A \rightarrow q\bar{q}X$ amplitude, and bring it to a form that will be easy to compare with the photon production amplitude. A straightforward use of the CGC rules (see [27, 28, 23, 24] for details and examples) gives for this amplitude the following sum of three terms⁴, each corresponding to a diagram in figure 1:

$$\begin{aligned}
\mathcal{M}_{DIS}^\mu(\mathbf{k}|\mathbf{q},\mathbf{p}) = & -i \int d^2\mathbf{x}_{2\perp} e^{i(\mathbf{q}_\perp + \mathbf{p}_\perp - \mathbf{k}_\perp) \cdot \mathbf{x}_{2\perp}} (U^\dagger(\mathbf{x}_{2\perp}) - 1) \\
& \times \bar{u}(\mathbf{q}) \left[\frac{\gamma^\mu(\not{Q} - \not{K} + m)\gamma^-}{(Q - K)^2 - m^2 + i\epsilon} \right] v(\mathbf{p}) \\
& + i \int d^2\mathbf{x}_{1\perp} e^{i(\mathbf{q}_\perp + \mathbf{p}_\perp - \mathbf{k}_\perp) \cdot \mathbf{x}_{1\perp}} (U(\mathbf{x}_{1\perp}) - 1) \\
& \times \bar{u}(\mathbf{q}) \left[\frac{\gamma^-(\not{K} - \not{P} + m)\gamma^\mu}{(P - K)^2 - m^2 + i\epsilon} \right] v(\mathbf{p}) \\
& + i \int \frac{d^2\mathbf{l}_\perp}{(2\pi)^2} \int d^2\mathbf{x}_{1\perp} d^2\mathbf{x}_{2\perp} \\
& \times e^{i\mathbf{l}_\perp \cdot \mathbf{x}_{1\perp}} e^{i(\mathbf{p}_\perp + \mathbf{q}_\perp - \mathbf{k}_\perp - \mathbf{l}_\perp) \cdot \mathbf{x}_{2\perp}} (U(\mathbf{x}_{1\perp}) - 1) (U^\dagger(\mathbf{x}_{2\perp}) - 1) \\
& \times \bar{u}(\mathbf{q}) \left[\frac{\gamma^-(\not{Q} - \not{L} + m)\gamma^\mu(\not{Q} - \not{K} - \not{L} + m)\gamma^-}{2p^-[(\mathbf{q}_\perp - \mathbf{l}_\perp)^2 + m^2 - 2q^-k^+] + 2q^-[(\mathbf{q}_\perp - \mathbf{k}_\perp - \mathbf{l}_\perp)^2 + m^2]} \right] v(\mathbf{p}) .
\end{aligned} \tag{3}$$

In this equation Q, P and K are the momenta of the outgoing quark, outgoing antiquark and incoming photon respectively, $\mathbf{x}_{1\perp}$ and $\mathbf{x}_{2\perp}$ are the coordinates in impact parameter space of the quark and antiquark. In the third diagram, the momentum L is the momentum transferred between the nucleus and the quark line. Its $-$ component is zero because the nucleus is moving at the speed of light in the $+z$ direction, and its $+$ component has already been integrated out by using the theorem of residues (we pick the pole in the upper half-plane, at $l^+ = q^+ - [(\mathbf{q}_\perp - \mathbf{l}_\perp)^2 + m^2 - i\epsilon]/2q^-$).

At this point, it is useful to note that since P and Q are on-shell, we have the following two identities:

$$\begin{aligned}
\bar{u}(\mathbf{q}) &= \frac{1}{2q^-} \bar{u}(\mathbf{q}) \gamma^- (m + \not{Q}) , \\
v(\mathbf{p}) &= -\frac{1}{2p^-} (m - \not{P}) \gamma^- v(\mathbf{p}) .
\end{aligned} \tag{4}$$

Inserting them respectively in the first and second term of Eq. (3), and introducing also a dummy variable \mathbf{l}_\perp via $\int d^2\mathbf{x}_{1\perp} d^2\mathbf{l}_\perp / (2\pi)^2 \exp(i\mathbf{l}_\perp \cdot \mathbf{x}_{1\perp})$ or $\int d^2\mathbf{x}_{2\perp} d^2\mathbf{l}_\perp / (2\pi)^2 \exp(i\mathbf{l}_\perp \cdot \mathbf{x}_{2\perp})$, we can combine three terms into one:

$$\mathcal{M}_{DIS}^\mu(\mathbf{k}|\mathbf{q},\mathbf{p}) = \frac{i}{2} \int \frac{d^2\mathbf{l}_\perp}{(2\pi)^2} \int d^2\mathbf{x}_{1\perp} d^2\mathbf{x}_{2\perp}$$

⁴The factor $2\pi\delta(k^- - p^- - q^-)$, which expresses the fact that the problem is invariant under translations in x^+ has been excluded from the definition of the amplitude \mathcal{M}^μ .

$$\begin{aligned} & \times e^{i\mathbf{l}_\perp \cdot \mathbf{x}_{1\perp}} e^{i(\mathbf{p}_\perp + \mathbf{q}_\perp - \mathbf{k}_\perp - \mathbf{l}_\perp) \cdot \mathbf{x}_{2\perp}} (U(\mathbf{x}_{1\perp})U^\dagger(\mathbf{x}_{2\perp}) - 1) \\ & \times \bar{u}(\mathbf{q}) \Gamma^\mu(k^\pm, \mathbf{k}_\perp | q^-, p^-, \mathbf{q}_\perp - \mathbf{l}_\perp) v(\mathbf{p}), \end{aligned} \quad (5)$$

where we denote

$$\begin{aligned} \Gamma^\mu(k^\pm, \mathbf{k}_\perp | q^-, p^-, \mathbf{q}_\perp - \mathbf{l}_\perp) & \equiv \\ & \equiv \frac{\gamma^-(\not{Q} - \not{L} + m) \gamma^\mu (\not{Q} - \not{K} - \not{L} + m) \gamma^-}{p^- [(q_\perp - l_\perp)^2 + m^2 - 2q^- k^+] + q^- [(q_\perp - k_\perp - l_\perp)^2 + m^2]}. \end{aligned} \quad (6)$$

This is our final expression for the DIS amplitude off the target color field. Note that Γ^μ a priori depends on \mathbf{p}_\perp and \mathbf{q}_\perp . However, in its list of arguments, we have anticipated the fact that the \mathbf{p}_\perp and \mathbf{q}_\perp that comes from the spinors drops out in physical quantities, because in the squared amplitude they always appear in combinations such as $\gamma^- u(\mathbf{q}) \bar{u}(\mathbf{q}) \gamma^- = 2q^- \gamma^-$. In Eq. (5), Γ^μ is a quantity which describes how the virtual photon splits into a $q\bar{q}$ pair, which longitudinal momenta q^-, p^- and transverse momentum of the quark $\mathbf{q}_\perp - \mathbf{l}_\perp$, while the factor $U(\mathbf{x}_{1\perp})U^\dagger(\mathbf{x}_{2\perp}) - 1$ can be seen as the scattering amplitude of the dipole on color field of the nucleus.

2.2 DIS Cross-section

From Eq. (5), one can obtain the γ^*A cross-section as

$$\begin{aligned} d\sigma_{DIS} &= \frac{d^3\mathbf{q}}{(2\pi)^2 2q_0} \frac{d^3\mathbf{p}}{(2\pi)^3 2p_0} \frac{1}{2k^-} 2\pi \delta(k^- - p^- - q^-) \\ & \times \langle \mathcal{M}_{DIS}^\mu(\mathbf{k}|\mathbf{q}, \mathbf{p}) \mathcal{M}_{DIS}^{\nu*}(\mathbf{k}|\mathbf{q}, \mathbf{p}) \rangle_\rho \epsilon_\mu(K) \epsilon_\nu^*(K), \end{aligned} \quad (7)$$

where $\langle \cdots \rangle_\rho$ denotes the average over the color sources and where $\epsilon^\mu(K)$ is the polarization vector of the photon. At this point, in order to exploit the fact that Γ^μ depends only on $\mathbf{m}_\perp \equiv \mathbf{q}_\perp - \mathbf{l}_\perp$, we can use this quantity as the integration variable in \mathcal{M}_{DIS}^μ , and we can integrate out trivially the transverse momenta \mathbf{q}_\perp and \mathbf{p}_\perp of the quark and antiquark in the final state, in order to obtain⁵:

$$\begin{aligned} \sigma_{DIS} &= \frac{1}{32\pi k_-^2} \int_0^1 \frac{dz}{z(1-z)} \int d^2\mathbf{r}_\perp \int \frac{d^2\mathbf{m}_\perp}{(2\pi)^2} \frac{d^2\mathbf{m}'_\perp}{(2\pi)^2} \epsilon_\mu(k) \epsilon_\nu^*(k) \\ & \times e^{i(\mathbf{m}_\perp - \mathbf{m}'_\perp) \cdot \mathbf{r}_\perp} \int d^2\mathbf{X}_\perp \text{Tr}_c \left(1 - \text{Re} \left\langle U(\mathbf{X}_\perp + \frac{\mathbf{r}_\perp}{2}) U^\dagger(\mathbf{X}_\perp - \frac{\mathbf{r}_\perp}{2}) \right\rangle_\rho \right) \\ & \times \text{Tr}_d \left((\not{q} + m) \Gamma^\mu(k^\pm, \mathbf{k}_\perp | q^-, p^-, \mathbf{m}_\perp) (\not{p} - m) \Gamma^{\nu\dagger}(k^\pm, \mathbf{k}_\perp | q^-, p^-, \mathbf{m}'_\perp) \right), \end{aligned} \quad (8)$$

with z the momentum fraction $z \equiv q^-/k^-$ ($p^- = (1-z)k^-$), where Tr_c denotes the color trace and Tr_d the Dirac trace, and where we have introduced the dipole

⁵We have made explicit the fact that it is the real part of the correlator $\langle \cdots \rangle_\rho$ which appears in the total cross-section, in order to emphasize the connection with the optical theorem. However, the real part has no effect since this correlator is purely real in the Color Glass Condensate model. Therefore, we drop it in the following formulas.

size $\mathbf{r}_\perp \equiv \mathbf{x}_{1\perp} - \mathbf{x}_{2\perp}$ and barycenter $\mathbf{X}_\perp \equiv (\mathbf{x}_{1\perp} + \mathbf{x}_{2\perp})/2$. If we introduce the dipole cross-section⁶

$$\sigma_{\text{dipole}}(\mathbf{r}_\perp) \equiv \frac{2}{N_c} \int d^2 \mathbf{X}_\perp \text{Tr}_c \left\langle 1 - U(\mathbf{X}_\perp + \frac{\mathbf{r}_\perp}{2}) U^\dagger(\mathbf{X}_\perp - \frac{\mathbf{r}_\perp}{2}) \right\rangle_\rho \quad (9)$$

and the square of the photon wave function:

$$\begin{aligned} |\Psi(k^\pm, \mathbf{k}_\perp | z, \mathbf{r}_\perp)|^2 &\equiv \frac{N_c \epsilon_\mu(K) \epsilon_\nu^*(K)}{64\pi k_\perp^2 z(1-z)} \int \frac{d^2 \mathbf{m}_\perp}{(2\pi)^2} \frac{d^2 \mathbf{m}'_\perp}{(2\pi)^2} e^{i(\mathbf{m}_\perp - \mathbf{m}'_\perp) \cdot \mathbf{r}_\perp} \\ &\times \text{Tr}_d \left((\not{q} + m) \Gamma^\mu(k^\pm, \mathbf{k}_\perp | q^-, p^-, \mathbf{m}_\perp) (\not{q} - m) \Gamma^{\nu\dagger}(k^\pm, \mathbf{k}_\perp | q^-, p^-, \mathbf{m}'_\perp) \right), \end{aligned} \quad (10)$$

we can write the following well known formula for the $\gamma^* A$ cross-section:

$$\sigma_{DIS} = \int_0^1 dz \int d^2 \mathbf{r}_\perp |\Psi(k^\pm, \mathbf{k}_\perp | z, \mathbf{r}_\perp)|^2 \sigma_{\text{dipole}}(\mathbf{r}_\perp). \quad (11)$$

So far, we have treated the scattering of the quark and antiquark off the nucleus at a purely classical level, and disregarded its energy dependence. This energy dependence is usually encoded in the dependence upon the variable $X \equiv -K^2/2K \cdot P_n$ where P_n is the 4-momentum of a nucleon inside the nucleus⁷. In the CGC model, this energy dependence is expected to arise in the functional which is used in order to perform the average over the sources, when one solves the renormalization group equation that controls its x -dependence.

2.3 Models for the dipole cross-section

2.3.1 McLerran-Venugopalan model

A first possibility to estimate the dipole cross-section is to use the McLerran-Venugopalan model, i.e. to use a Gaussian distribution of the sources $\rho_a(z^-, \mathbf{z}_\perp)$ that contribute to the matrix $U(\mathbf{x}_\perp)$ defined in Eq. (2). Assuming a distribution of the form

$$W[\rho] \equiv \exp \left\{ - \int dx^- d^2 \mathbf{x}_\perp \frac{\rho_a(x^-, \mathbf{x}_\perp) \rho_a(x^-, \mathbf{x}_\perp)}{2\mu^2(x^-, \mathbf{x}_\perp)} \right\}, \quad (12)$$

⁶Strictly speaking, the dipole cross-section should depend on the longitudinal momentum fractions z and $1-z$ of the quark and antiquark, because these parameters control the rapidity interval between the quark or antiquark and the target. However, the small x evolution that we will consider later aims at resumming leading powers of $\ln(1/x)$, which means that we neglect $\ln(1/z)$ and $\ln(1/(1-z))$ in front of $\ln(1/x)$. This is a reasonable approximation at high energy (small x) and if the photon wave function does not overweight values of z close to 0 or 1.

⁷At leading twist, and in the frame where the DIS can be seen as a quark of the nucleus being struck by the virtual photon, x has the interpretation of the longitudinal momentum fraction of the struck quark.

with $\mu^2(x^-, \mathbf{x}_\perp)$ a density of color sources per unit volume, one obtains (see the appendix A of [27]):

$$\sigma_{\text{dipole}}(\mathbf{r}_\perp) = \pi R^2 \left[1 - \exp \left(-Q_s^2 \int d^2 \mathbf{z}_\perp [G_0(\mathbf{z}_\perp) - G_0(\mathbf{z}_\perp - \mathbf{r}_\perp)]^2 \right) \right], \quad (13)$$

where $Q_s^2 \sim \alpha_s^2 \int dz^- \mu^2(z^-)$ (in order to arrive at this formula for the dipole cross-section, one has to assume that the target is homogeneous in the transverse plane) and where G_0 is the free propagator in two dimensions:

$$G_0(\mathbf{z}_\perp) = \int \frac{d^2 \mathbf{k}_\perp}{(2\pi)^2} \frac{e^{i\mathbf{k}_\perp \cdot \mathbf{z}_\perp}}{\mathbf{k}_\perp^2} = \frac{1}{4\pi} \ln \left(\frac{1}{\mathbf{z}_\perp^2 \Lambda^2} \right), \quad (14)$$

where Λ is some infrared cutoff related to the scale at which color neutrality occurs. Therefore, Λ is at least as large as the inverse hadron size, i.e. Λ_{QCD} . In fact, it can be proven that in a saturated target, color neutrality occurs over transverse spatial scales as small as Q_s^{-1} [19, 29]. At small dipole sizes, this integral behaves like $r_\perp^2 \ln(1/r_\perp \Lambda)$. Quantum corrections to the McLerran-Venugopalan model give an x dependence to the saturation scale Q_s and hence to the dipole cross-section [9, 10, 17, 18, 19, 20, 30, 31].

2.3.2 Golec-Biernat-Wüsthoff model - without evolution

In [32, 33, 34], Golec-Biernat and Wüsthoff developed a model of dipole cross-section that is loosely inspired by the previous form of the dipole cross-section:

$$\sigma_{\text{dipole}}(x, \mathbf{r}_\perp) = \sigma_0 (1 - \exp(-r_\perp^2 / 4R_0^2(x))) , \quad (15)$$

with $R_0^2(x) [\text{GeV}^{-2}] = (x/x_0)^\lambda$. The main simplification compared to Eq. (13) is that the \mathbf{r}_\perp dependence is taken to be strictly Gaussian, i.e. one neglects the slowly varying logarithm in the exponential⁸. The x dependence is reminiscent of the BFKL evolution of the gluon structure function at small x . Then, in order to determine the values of the three parameters σ_0 , λ and x_0 , they fitted the DIS data at HERA for $x < 0.01$. The best fit was obtained with $\sigma_0 = 23\text{mb}$, $\lambda = 0.29$ and $x_0 = 3.10^{-4}$.

2.3.3 Bartels-Golec-Biernat-Kowalski model - with evolution

The previous model for the dipole cross-section was subsequently improved in [35] in order to make the small dipole limit agree with leading twist perturbative QCD, including the DGLAP evolution of the gluon density. This new model

⁸When we connect particle production in pA collisions to the dipole cross-section in section 4, we will show that this Gaussian form fails to reproduce the standard perturbative result for the p_\perp spectrum of the produced particles. In other words, while this logarithm is not crucial in order to obtain a reasonable fit of small- x DIS data, it is crucial in order to get the correct spectrum shape in pA collisions.

improves the agreement with the high Q^2 data (up to $Q^2 \leq 450 \text{ GeV}^2$). In this version the dipole-proton cross section is [35] (see also [36]):

$$\sigma_{\text{dipole}}(\mathbf{r}_\perp, x) = \sigma_0 \left[1 - \exp \left\{ - \frac{\pi^2 r_\perp^2 \alpha_s(\mu^2) x G(x, \mu^2)}{3\sigma_0} \right\} \right] \quad (16)$$

where $\mu^2 \equiv \mu_0^2 + C/r_\perp^2$ and all the parameters are determined from fits to the DIS data from HERA. Using Eq. (16) in (11) gives the cross section for the interaction of a virtual photon with a proton target described by the Color Glass Condensate. Since we are interested in scattering off a nucleus target, we can replace $xG(x, \mu^2)$ in Eq. (16) by $AxG(x, \mu^2)$. The parameter σ_0 must also be scaled according to the transverse area of the target.

The goal of the rest of this paper is to show that once one knows the dipole cross-section, there are several other interesting processes for which one can make quantitative predictions, since they can be expressed in terms of the same dipole cross-section. For instance, the cross section for jet production in pA collisions is very closely related to the dipole cross-section on a nucleus, as we will see in section 4.

3 Virtual photon production in pA collisions

3.1 Photon production amplitude

The first example we consider is the production of virtual photons (or, equivalently, lepton pairs) in pA collisions, since this is in fact the process which is the most closely related to DIS. We follow here the description of the proton assumed in [23, 24], where it was assumed that the proton can be described in terms of standard parton distributions. Therefore, the relevant subprocess for the production of a virtual photon in pA is $qA \rightarrow q\gamma^*X$, which is related to $\gamma^*A \rightarrow q\bar{q}X$ by a crossing symmetry.

The main difference in the case of γ^* production is the fact that there are only two diagrams, represented in figure 2. Note that there could a priori be a

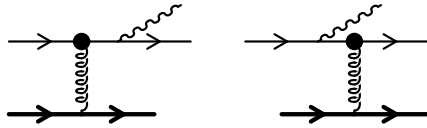


Figure 2: The relevant diagrams for $qA \rightarrow q\gamma^*X$ in the Color Glass Condensate model. The black dots denote the eikonal interaction between the quark or antiquark with the classical color field.

third diagram with eikonal interactions of the quark both before and after the photon emission. However, this diagram is in fact strongly suppressed by large energy denominators [23], which simply indicates that by the time the photon

has been emitted after a first scattering of the quark off the nucleus, the nucleus is far behind and any further scattering is impossible (in order words, the nucleus is so fast that the photon is emitted outside of the nucleus). This discrepancy between the number of diagrams contributing to both processes is what makes the correspondence between the two non-trivial⁹, and worth checking explicitly. In the CGC model, the $qA \rightarrow q\gamma^*X$ amplitude is given by¹⁰

$$\begin{aligned} \mathcal{M}_{\gamma^*}^\mu(\mathbf{p}|\mathbf{q}, \mathbf{k}) &= i \int d^2\mathbf{x}_\perp e^{i(\mathbf{q}_\perp + \mathbf{k}_\perp - \mathbf{p}_\perp) \cdot \mathbf{x}_\perp} (U(\mathbf{x}_\perp) - 1) \\ &\times \bar{u}(\mathbf{q}) \left[\frac{\gamma^\mu(\not{Q} + \not{K} + m)\gamma^-}{(Q + K)^2 - m^2 + i\epsilon} + \frac{\gamma^-(\not{P} - \not{K} + m)\gamma^\mu}{(P - K)^2 - m^2 + i\epsilon} \right] u(\mathbf{p}), \end{aligned} \quad (17)$$

where the two terms correspond to the two diagrams of figure 2 respectively. In this equation p, q and k are the momenta of the incoming quark, and of the outgoing quark and photon respectively, and \mathbf{x}_\perp is the transverse coordinate of the quark. Using now the first of Eqs. (4) as well as

$$u(\mathbf{p}) = \frac{1}{2p^-} (m + \not{P}) \gamma^- u(\mathbf{p}), \quad (18)$$

and introducing again a dummy variable \mathbf{l}_\perp , we can after some algebra rewrite the γ^* production amplitude as:

$$\begin{aligned} \mathcal{M}_{\gamma^*}^\mu(\mathbf{p}|\mathbf{q}, \mathbf{k}) &= \frac{i}{2} \int \frac{d^2\mathbf{l}_\perp}{(2\pi)^2} \int d^2\mathbf{x}_{1\perp} d^2\mathbf{x}_{2\perp} \\ &\times e^{i\mathbf{l}_\perp \cdot \mathbf{x}_{1\perp}} e^{i(\mathbf{q}_\perp + \mathbf{k}_\perp - \mathbf{p}_\perp - \mathbf{l}_\perp) \cdot \mathbf{x}_{2\perp}} (U(\mathbf{x}_{1\perp}) - U(\mathbf{x}_{2\perp})) \\ &\times \bar{u}(\mathbf{q}) \Gamma^\mu(-k^\pm, -\mathbf{k}_\perp | q^-, -p^-, \mathbf{q}_\perp - \mathbf{l}_\perp) u(\mathbf{p}), \end{aligned} \quad (19)$$

where Γ^μ is again the function defined by Eq. (6). We see that the only difference between the DIS and γ^* -production amplitudes, besides the obvious changes $P \rightarrow -P$ and $K \rightarrow -K$, is an extra factor $U^\dagger(\mathbf{x}_{2\perp})$ under the integral. In other words, the two amplitudes can be related by crossing symmetry up to a unitary matrix, which violates a strict crossing symmetry at the amplitude level. This has been noted independently by S. Peigné in [38], where Drell-Yan and DIS are compared up to the terms involving three scatterings on the target. In the present case, this violation is in fact due to the eikonal approximation. Indeed, this approximation being valid for an asymptotically large relative momentum between the projectile and the target, it does not allow to reverse continuously the momentum of the projectile.

⁹If we were working at fixed order $\mathcal{O}(\alpha_s)$ instead of resumming all the eikonal interactions, only the first two diagrams of figure 1 would contribute to DIS, and finding the relation between DIS and γ^* production would be trivial. Note that a similar correspondence was found in [28], although in a case where the photon kinematics was far less general.

¹⁰Again, we do not include the factor $2\pi\delta(p^- - q^- - k^-)$ in the definition of $\mathcal{M}_{\gamma^*}^\mu$.

3.2 Cross-section

The photon production cross-section is obtained from the amplitude by

$$d\sigma_{\gamma^*} = \frac{d^3\mathbf{q}}{(2\pi)^2 2q_0} \frac{d^3\mathbf{k}}{(2\pi)^3 2k_0} \frac{1}{2p^-} 2\pi\delta(p^- - q^- - k^-) \\ \times \frac{1}{2N_c} \langle \mathcal{M}_{\gamma^*}^\mu(\mathbf{p}|\mathbf{q}, \mathbf{k}) \mathcal{M}_{\gamma^*}^{\nu*}(\mathbf{p}|\mathbf{q}, \mathbf{k}) \rangle_\rho \epsilon_\mu(K) \epsilon_\nu^*(K), \quad (20)$$

where the factor $1/2N_c$ is for the average over the color and spin of the incoming quark. At this point, it is useful to replace the integration variable \mathbf{l}_\perp by $\mathbf{m}_\perp = \mathbf{q}_\perp - \mathbf{l}_\perp$ both in the amplitude and in its complex conjugate, in order to exploit the momentum dependence of the function Γ^μ . Another simplification comes from the fact that any term in the amplitude squared depends non-trivially only on two out of the four transverse coordinates. Therefore, the two transverse coordinates that appear only in exponentials can be integrated out immediately, which gives two delta constraints on some combination of transverse momenta, that can be used in order to perform the integrals over \mathbf{m}_\perp and \mathbf{m}'_\perp . Following this procedure, one obtains the following form for the differential γ^* production cross-section¹¹:

$$d\sigma_{\gamma^*} = \frac{d^3\mathbf{q}}{(2\pi)^3 2q_0} \frac{d^3\mathbf{k}}{(2\pi)^3 2k_0} \frac{1}{2p^-} 2\pi\delta(p^- - q^- - k^-) \\ \times \int d^2\mathbf{r}_\perp e^{i(\mathbf{q}_\perp + \mathbf{k}_\perp - \mathbf{p}_\perp) \cdot \mathbf{r}_\perp} \int d^2\mathbf{X}_\perp \text{Tr}_c \left\langle 1 - U(\mathbf{X}_\perp + \frac{\mathbf{r}_\perp}{2}) U^\dagger(\mathbf{X}_\perp - \frac{\mathbf{r}_\perp}{2}) \right\rangle_\rho \\ \times \frac{1}{2N_c} \left[M(\mathbf{p}_\perp - \mathbf{k}_\perp, \mathbf{p}_\perp - \mathbf{k}_\perp) + M(\mathbf{q}_\perp, \mathbf{q}_\perp) \right. \\ \left. - M(\mathbf{q}_\perp, \mathbf{p}_\perp - \mathbf{k}_\perp) - M(\mathbf{p}_\perp - \mathbf{k}_\perp, \mathbf{q}_\perp) \right], \quad (21)$$

where we use the shorthand

$$M(\mathbf{m}_\perp, \mathbf{m}'_\perp) \equiv \epsilon_\mu(K) \epsilon_\nu^*(K) \text{Tr}_d((\not{q} + m) \Gamma^\mu(-k^\pm, -\mathbf{k}_\perp | q^-, -p^-, \mathbf{m}_\perp) \\ \times (\not{p} + m) \Gamma^{\nu\dagger}(-k^\pm, -\mathbf{k}_\perp | q^-, -p^-, \mathbf{m}'_\perp)). \quad (22)$$

In fact, the four terms in Eq. (21) could have been obtained directly by squaring the two terms of Eq. (17)¹². Again, we see that the dipole cross-section appears naturally in this cross-section. Therefore, if one determines the dipole cross-section from DIS data, then it becomes possible to make quantitative *predictions* for the production of virtual photons in pA collisions. This possibility has already been exploited in [26] in order to study nuclear effects on the Drell-Yan process.

¹¹We also use the freedom to add a constant to the term in UU^\dagger , because doing this does not change the final result for the cross-section.

¹²The form of Eq. (19) for the γ^* production amplitude is in fact not optimal in order to calculate the cross-section because it contains some redundant variables. Its only advantage is to make obvious the similarities with the DIS amplitude.

One can in fact obtain a form very similar to Eq. (11) for the γ^* production cross-section integrated over the transverse momenta \mathbf{q}_\perp and \mathbf{k}_\perp of the final particles:

$$\sigma_{\gamma^*} = \int_0^1 dz \int d^2 \mathbf{r}_\perp |\phi(p^-, \mathbf{p}_\perp | k^+, z, \mathbf{r}_\perp)|^2 \sigma_{\text{dipole}}(\mathbf{r}_\perp), \quad (23)$$

where z is the longitudinal momentum fraction taken by the photon ($k^- = zp^-$, $q^- = (1-z)p^-$) and where we denote

$$\begin{aligned} |\phi(p^-, \mathbf{p}_\perp | k^+, z, \mathbf{r}_\perp)|^2 &\equiv \frac{1}{64\pi p_-^2 z(1-z)} \int \frac{d^2 \mathbf{q}_\perp}{(2\pi)^2} \int \frac{d^2 \mathbf{k}_\perp}{(2\pi)^2} e^{i(\mathbf{q}_\perp + \mathbf{k}_\perp - \mathbf{p}_\perp) \cdot \mathbf{r}_\perp} \\ &\times \left[M(\mathbf{p}_\perp - \mathbf{k}_\perp, \mathbf{p}_\perp - \mathbf{k}_\perp) + M(\mathbf{q}_\perp, \mathbf{q}_\perp) \right. \\ &\quad \left. - M(\mathbf{q}_\perp, \mathbf{p}_\perp - \mathbf{k}_\perp) - M(\mathbf{p}_\perp - \mathbf{k}_\perp, \mathbf{q}_\perp) \right]. \end{aligned} \quad (24)$$

4 Forward pion production in pA collisions

4.1 Quark scattering amplitude

In this section we show how one can relate the cross section for forward particle production in pA collisions to the dipole cross-section. To be specific, we will consider pions but this can be repeated for any particle for which there is a known fragmentation function. We will use the results of [21, 22] for scattering of an on-shell quark from the target described by the Color Glass Condensate.

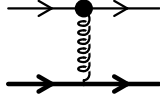


Figure 3: The relevant diagram for $qA \rightarrow qX$ in the Color Glass Condensate model. The black dots denote the eikonal interaction between the quark or antiquark with the classical color field.

The amplitude for scattering of a quark from the target described by a classical field is given by the diagram represented in figure 3, and has been obtained in [21, 22]. Factoring out the obvious $2\pi\delta(p^- - q^-)$, this amplitude reads (the same as Eq. (1)):

$$\mathcal{M}_{qA \rightarrow qX}(\mathbf{p}|\mathbf{q}) = \bar{u}(\mathbf{q}) \left[\gamma^- \int d^2 \mathbf{x}_\perp e^{i(\mathbf{q}_\perp - \mathbf{p}_\perp) \cdot \mathbf{x}_\perp} (U(\mathbf{x}_\perp) - 1) \right] u(\mathbf{p}), \quad (25)$$

where \mathbf{p} and \mathbf{q} are the momenta of the incoming and outgoing quark respectively.

4.2 Scattering cross section

From this amplitude, it is easy to obtain the cross section [21, 22]:

$$d\sigma_{qA \rightarrow qX} = \frac{d^3\mathbf{q}}{(2\pi)^3 2q_0} \frac{1}{2p^-} 2\pi\delta(p^- - q^-) \frac{1}{2N_c} \langle \mathcal{M}_{qA \rightarrow qX}(\mathbf{p}|\mathbf{q}) \mathcal{M}_{qA \rightarrow qX}^*(\mathbf{p}|\mathbf{q}) \rangle_\rho, \quad (26)$$

where the prefactor $1/2N_c$ comes from the average over the spin and color of the incoming quark. This can be rewritten as:

$$d\sigma_{qA \rightarrow qX} = \frac{d^2\mathbf{q}_\perp}{(2\pi)^2} \frac{1}{N_c} \int d^2\mathbf{r}_\perp e^{i(\mathbf{q}_\perp - \mathbf{p}_\perp) \cdot \mathbf{r}_\perp} \times \int d^2\mathbf{X}_\perp \text{Tr}_c \left\langle \left(U(\mathbf{X}_\perp + \frac{\mathbf{r}_\perp}{2}) - 1 \right) \left(U^\dagger(\mathbf{X}_\perp - \frac{\mathbf{r}_\perp}{2}) - 1 \right) \right\rangle_\rho. \quad (27)$$

Note that for the scattering of a gluon, one would have to replace the matrix U by its analogue in the adjoint representation, but the average over the color of the initial state would require a factor $1/(N_c^2 - 1)$ instead of $1/N_c$. Expanding the correlator in the bracket $\langle \cdots \rangle_\rho$, we can rewrite this cross-section in terms of the dipole cross-section:

$$d\sigma_{qA \rightarrow qX} = \frac{d^2\mathbf{q}_\perp}{(2\pi)^2} dq^- \delta(q^- - p^-) \int d^2\mathbf{r}_\perp e^{i\mathbf{q}_\perp \cdot \mathbf{r}_\perp} \times \left[\frac{1}{N_c} \int d^2\mathbf{X}_\perp \text{Tr}_c \left\langle 2 - U(\mathbf{X}_\perp + \frac{\mathbf{r}_\perp}{2}) - U^\dagger(\mathbf{X}_\perp - \frac{\mathbf{r}_\perp}{2}) \right\rangle_\rho - \sigma_{\text{dipole}}(\mathbf{r}_\perp) \right], \quad (28)$$

where, anticipating the use of collinear factorization for the incoming quark, we have set $\mathbf{p}_\perp = 0$. The first term $\langle 2 - U - U^\dagger \rangle_\rho$ is essential in order to obtain the correct total cross-section. Indeed, integrating over \mathbf{q}_\perp generates a $\delta(\mathbf{r}_\perp)$, and since $\sigma_{\text{dipole}}(\mathbf{r}_\perp = 0) = 0$, we have for the total $qA \rightarrow qX$ cross-section¹³:

$$\sigma_{qA \rightarrow qX}^{\text{total}} = \frac{1}{N_c} \int d^2\mathbf{X}_\perp \text{Tr}_c \langle 2 - U(\mathbf{X}_\perp) - U^\dagger(\mathbf{X}_\perp) \rangle_\rho. \quad (30)$$

If we recall (see [27] for instance) that $\langle U(\mathbf{x}_\perp) \rangle_\rho$ is suppressed exponentially like $\exp(-Q_s^2/\Lambda_{QCD}^2)$ when $Q_s \gg \Lambda_{QCD}$, we can approximate the $qA \rightarrow qX$ cross-section by:

$$d\sigma_{qA \rightarrow qX} = \frac{d^2\mathbf{q}_\perp}{(2\pi)^2} dq^- \delta(q^- - p^-) \int d^2\mathbf{r}_\perp e^{i\mathbf{q}_\perp \cdot \mathbf{r}_\perp} (2\pi R^2 - \sigma_{\text{dipole}}(\mathbf{r}_\perp)), \quad (31)$$

¹³In order for the optical theorem to hold, the forward elastic ($qA \rightarrow qA$) amplitude must be:

$$\mathcal{M}_{qA \rightarrow qA}^{\text{forward}} = 2p^- \int d^2\mathbf{x}_\perp \langle U(\mathbf{x}_\perp) - 1 \rangle_\rho. \quad (29)$$

In other words, the forward $qA \rightarrow qA$ amplitude is obtained from Eq. (25) by setting $\mathbf{p} = \mathbf{q}$ and by averaging the amplitude over the classical color sources in the nucleus.

for a target of radius R . The term in $2\pi R^2$ contributes only to the scattering in the forward direction (i.e. at $\mathbf{q}_\perp = 0$).

4.3 Discussion

4.3.1 Cronin effect at the partonic level

From the previous relations, it is trivial to write the non-forward part of the q_\perp -spectrum as:

$$\frac{d\sigma_{qA \rightarrow qX}}{d^2\mathbf{q}_\perp} = -\frac{1}{(2\pi)^2} \tilde{\sigma}_{\text{dipole}}(q_\perp), \quad (32)$$

where $\tilde{\sigma}_{\text{dipole}}(q_\perp)$ is the Fourier transform of the dipole cross-section, defined as:

$$\tilde{\sigma}_{\text{dipole}}(q_\perp) \equiv \int d^2\mathbf{r}_\perp e^{i\mathbf{q}_\perp \cdot \mathbf{r}_\perp} \sigma_{\text{dipole}}(\mathbf{r}_\perp). \quad (33)$$

In other words, the q_\perp -spectrum of particle production in pA collisions is given by the opposite of the Fourier transform of the dipole cross-section.

In the McLerran-Venugopalan model, this Fourier transform has been studied in detail in [27, 28] where it controls the production of $q\bar{q}$ pairs in ultra-peripheral AA collisions and was denoted $\pi R^2 C(\mathbf{q}_\perp)$ (see for instance the appendix B of [27]). In particular, the large q_\perp behavior of this function was found to be

$$C(\mathbf{q}_\perp) = 2 \frac{Q_s^2}{q_\perp^4} + \frac{8}{\pi} \frac{Q_s^4}{q_\perp^6} \left(\ln \left(\frac{q_\perp}{\Lambda_{QCD}} \right) - 1 \right) + \mathcal{O} \left(\frac{Q_s^6}{q_\perp^8} \right). \quad (34)$$

Note that if one replaces Q_s^2 by its expression in terms of parton distributions inside the target, the first term in $1/q_\perp^4$ reproduces the perturbative QCD result for $qg \rightarrow qg$ scattering with one gluon exchange in the t-channel (i.e. the dominant piece at high energy). In addition, if one assumes that Q_s^2 scales like $A^{1/3}$ for large nuclei, then the leading term of the q_\perp spectrum simply scales like A (another $A^{2/3}$ comes from the transverse area πR^2). If the second term in this expansion scales differently with A , then there is a Cronin effect. From Eq. (34), one can see that the next-to-leading term in the q_\perp -spectrum is scaling like $A^{4/3}$ and is positive. Therefore, one has a positive Cronin effect in the McLerran-Venugopalan model. The ratio $(A_{\text{ref}}/A) d\sigma_{qA \rightarrow qX} / d\sigma_{qA_{\text{ref}} \rightarrow qX}$, as predicted in the McLerran-Venugopalan model, is plotted as a function of q_\perp in figure 4. The reference nucleus is chosen such that the corresponding saturation scale is $Q_{s,\text{ref}}^2 = 1 \text{ GeV}^2$, and the ratio is displayed for two nuclei such that the saturation scales are $Q_s^2 = 2 \text{ GeV}^2$ and $Q_s^2 = 3 \text{ GeV}^2$. One can see that this ratio goes to 1 at large transverse momentum, and exhibits a pronounced maximum at intermediate q_\perp 's before dropping below 1 at small transverse momenta.

Alternatively, one could take $A_{\text{ref}} = A = 200$ and consider quark nucleus scattering at mid rapidity, assuming that $Q_{s,\text{ref}}^2 = 1 \text{ GeV}^2$ at mid rapidity. Then the solid and dashed lines correspond to the relative enhancement of the cross section in the forward rapidity region, $y \sim 2.5$ and $y \sim 3.5$ units away from mid rapidity (towards the proton), respectively. The low q_\perp spectrum is more

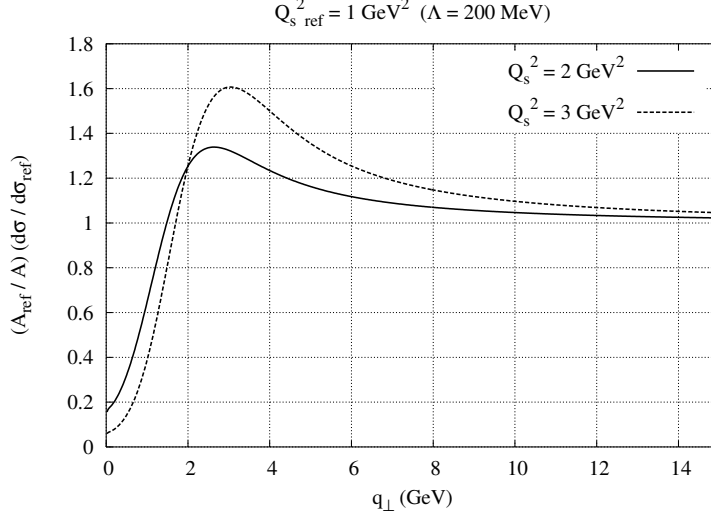


Figure 4: Cronin effect at the partonic level in the McLerran-Venugopalan model. The reference nucleus is chosen such that the corresponding saturation scale is $Q_{s\text{ref}}^2 = 1\text{GeV}^2$. This reference value of Q_s is compared to nuclei for which $Q_s^2 = 2\text{GeV}^2$ and $Q_s^2 = 3\text{GeV}^2$. The infrared cutoff is set to $\Lambda = 200\text{MeV}$.

suppressed as one goes to more forward rapidities and high q_\perp enhancement is stronger and moves to higher q_\perp .

It would be interesting to study whether this phenomenon is present in more sophisticated models of the dipole cross-section, like the model of Bartels, Golec-Biernat and Kowalski. It is also necessary to fold this “partonic level” calculation with the proton parton distribution functions, and with the appropriate fragmentation functions, as this could potentially suppress the effect. A numerical study of these issues is underway.

4.3.2 Further constraints of the dipole cross-section in pA

In DIS, one does not probe thoroughly the dipole cross-section, but only its overlap with the square of the photon wave function. This implies that some values of r_\perp matter more than others in the integral. One could therefore see Eq. (32) as another way of constraining the dipole cross-section. In particular, one would like to recover the results of perturbative QCD at large q_\perp , that is a cross-section that falls like q_\perp^{-4} (up to logarithms coming from the running α_s and from the DGLAP evolution of the gluon distribution inside the target).

For instance, this remark pretty much excludes the Golec-Biernat-Wüsthoff model of the dipole cross-section. Indeed, in this model (see Eq. (15)) the Fourier

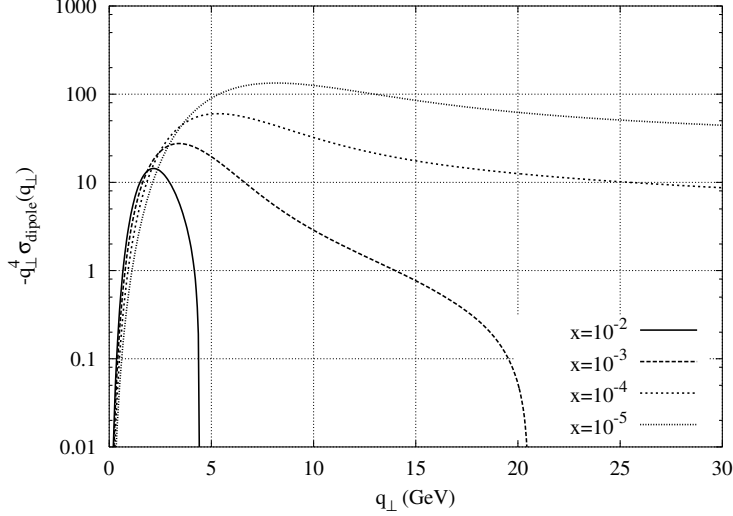


Figure 5: Values of $-q_{\perp}^4 \tilde{\sigma}_{\text{dipole}}(q_{\perp})$ as a function of q_{\perp} , for several values of x in the model of Bartels, Golec-Biernat and Kowalski.

transform that gives the q_{\perp} -spectrum can be performed analytically, giving:

$$\frac{d\sigma_{qA \rightarrow qX}}{d^2\mathbf{q}_{\perp}} = \frac{R_0^2(x)\sigma_0}{\pi} e^{-R_0^2(x)q_{\perp}^2}. \quad (35)$$

The major difference compared to the result in the McLerran-Venugopalan model is the large q_{\perp} behavior, which exhibits a Gaussian tail, as opposed to a power law tail. This fact alone is probably enough to justify not considering this model any further in order to study the region of large transverse momenta in pA collisions.

For the Bartels-Golec-Biernat-Kowalski model, one needs to compute numerically the Fourier transform of the dipole cross-section. In order to do this, we have taken the parameters of their second fit (“Fit 2” in Table 1 of [35]), which lead to the results displayed in figure 5. One can see that for very small values of x ($x = 10^{-4}, x = 10^{-5}$ on this plot) one obtains the expected scaling at large q_{\perp} . Indeed, q_{\perp}^4 times the Fourier transform of the dipole cross section is almost constant. However, for larger values of x ($x = 10^{-2}, x = 10^{-3}$ on the plot), the Fourier transform of the dipole cross-section suddenly drops at some q_{\perp} and its sign changes ¹⁴.

Above the q_{\perp} where this happens, one would obtain a negative $qA \rightarrow qX$ cross-section from formula Eq. (32). In this formula, one apparently probes different aspects of the dipole cross-section compared to DIS, and the model by Bartels, Golec-Biernat and Kowalski, although very successful at fitting all the

¹⁴This depends on whether a running or constant α_s is used [39]. For constant α_s one always gets a positive sign. See also eq. 20 in [35] and the discussion afterwards.

HERA DIS data at $x < 10^{-2}$, does not give a consistent answer for pA collisions at moderate x . Somehow, this defect is hidden in DIS by the way the photon wave functions weights the different values of r_{\perp} . Given this, one could perhaps reverse the main argument of this paper, and consider pA collisions as a way of either fine tuning the dipole model, or as a way of ruling it out.

4.4 From $qA \rightarrow qX$ to $pA \rightarrow \pi X$

To relate (31) to proton-nucleus collisions, we can use collinear factorization on the proton side and convolute (31) with the quark distribution function inside a proton and a quark-pion fragmentation function to get the cross section for $pA \rightarrow \pi X$.

$$\frac{d\sigma_{pA \rightarrow \pi(k)X}}{dk^- d^2\mathbf{k}_{\perp}} \equiv \int dx_q dz q_p(x_q) \frac{d\sigma_{qA \rightarrow qX}}{dq^- d^2\mathbf{q}_{\perp}} D_{q/\pi}(z) \quad (36)$$

where $q_p(x_q)$ is the distribution function of quarks with fractional momentum x_q inside a proton and $D_{q/\pi}(z)$ is the fragmentation function of a quark into a pion carrying fraction z of its energy. Using (31) in (36) we get

$$\begin{aligned} \frac{d\sigma_{pA \rightarrow \pi(y, \mathbf{k}_{\perp})X}}{dy d^2\mathbf{k}_{\perp}} &= \frac{1}{(2\pi)^2} \sqrt{\frac{k_{\perp}^2}{s}} e^y \int_{z_{\min}}^1 dz q_p(x_q) D_{q/\pi}(z) \\ &\times \int d^2\mathbf{r}_{\perp} e^{i\mathbf{k}_{\perp} \cdot \mathbf{r}_{\perp}/z} (2\pi R^2 - \sigma_{\text{dipole}}(\mathbf{r}_{\perp}, x_g)), \end{aligned} \quad (37)$$

where we have used the following kinematical relations $x_q = k_{\perp} e^y / z \sqrt{s}$, $x_g = k_{\perp} e^{-y} / z \sqrt{s}$, $z_{\min} = k_{\perp} e^y / \sqrt{s}$ (\sqrt{s} is the center of mass energy for a *proton-nucleon subsystem*). This way one can relate production of pions, kaons, protons, neutrons, photons and dileptons in proton-nucleus collisions in the forward rapidity region to the structure functions measured in DIS. For this approach to be self-consistent, one needs to make sure that the dominant contribution to (37) comes from the small x (≤ 0.01) region. Our preliminary result seem to indicate that this is indeed the case. A detailed numerical study of particle production in proton-nucleus collisions at RHIC is currently underway and will be reported elsewhere.

5 Conclusions

In this paper, we have shown that in a classical description of the gluon content of the nucleus, there are many interesting physical quantities that can be related to the dipole cross-section (or, at a more formal level, to the correlator $\langle U(0)U^{\dagger}(\mathbf{x}_{\perp}) \rangle$ of two Wilson lines). This was already known for deep inelastic scattering and for the Drell-Yan process when one considers cross-sections integrated over the phase-space of the final state. In this paper, we establish also a similar correspondence for forward particle production in proton nucleus collisions, this time for the differential cross-section. More precisely, we show that

the q_\perp spectrum of the produced particles is related to the Fourier transform of the dipole cross-section.

At a more formal level, we have generalized the standard leading twist collinear factorization approach to calculation of hadronic cross sections by showing that there is a universal object, the quark antiquark dipole cross section, which appears in all particle production cross sections in high energy proton-nucleus collisions. This dipole cross section plays the role of leading twist parton distributions in an all twist environment. In principle, it can be measured in DIS or for example, in single inclusive pion production in high energy proton-nucleus collisions. Once it is measured in a given process, it can be used to predict cross sections for other processes such as single inclusive hadron, jet, photon or dilepton production in high energy proton-nucleus collisions.

This result could therefore be used in order to make predictions for pA collisions, or to further constrain (or to rule out) the dipole model with proton-nucleus experiments. The detailed numerical study needed in order to make quantitative statements is in progress and will be presented in a future work [40]. However, a preliminary investigation of the Fourier transform of the dipole cross-section in the model of [35] seem to lead to a negative $qA \rightarrow qX$ differential cross-section for some values of x at large q_\perp . This suggests that the small r_\perp improvement of the dipole cross-section made in [35] over [32, 33] is still not quite able to ensure that the results of perturbative QCD are recovered at large transverse momentum.

Acknowledgment

We thank A. Dumitru, E. Iancu, K. Itakura, S. Jeon, Y. Kovchegov, H. Kowalski, S. Peigné, D. Teaney, R. Venugopalan and W. Vogelsang for useful discussions. We would also like to thank H. Kowalski for providing us with his code for calculating the dipole cross section in the Bartels-Golec-Biernat-Kowalski model, and L. Schoeffel for providing us with his code of DGLAP evolution. J.J-M. is supported by the U.S. Department of Energy under Contract No. DE-AC02-98CH10886 and in part by a PDF from BSA and would like to acknowledge the hospitality of SUNY Stony Brook nuclear theory group while this work was being completed. F.G. would like to thank the LPT/Orsay where part of this work has been performed.

References

- [1] L.V. Gribov, E.M. Levin, M.G. Ryskin, Phys. Rept. **100**, 1 (1983).
- [2] A.H. Mueller, J-W. Qiu, Nucl. Phys. **B 268**, 427 (1986).
- [3] L. McLerran, R. Venugopalan, Phys. Rev. **D 49**, 2233 (1994).
- [4] L. McLerran, R. Venugopalan, Phys. Rev. **D 49**, 3352 (1994).

- [5] L. McLerran, R. Venugopalan, Phys. Rev. **D 59**, 094002 (1999).
- [6] Yu.V. Kovchegov, Phys. Rev. **D 54**, 5463 (1996).
- [7] Yu.V. Kovchegov, Phys. Rev. **D 55**, 5445 (1997).
- [8] J. Jalilian-Marian, A. Kovner, L. McLerran, H. Weigert, Phys. Rev. **D 55**, 5414 (1997).
- [9] J. Jalilian-Marian, A. Kovner, A. Leonidov, H. Weigert, Nucl. Phys. **B 504**, 415 (1997).
- [10] J. Jalilian-Marian, A. Kovner, A. Leonidov, H. Weigert, Phys. Rev. **D 59**, 014014 (1999).
- [11] J. Jalilian-Marian, A. Kovner, A. Leonidov, H. Weigert, Phys. Rev. **D 59**, 034007 (1999).
- [12] J. Jalilian-Marian, A. Kovner, H. Weigert, Phys. Rev. **D 59**, 014015 (1999).
- [13] A. Ayala, J. Jalilian-Marian, L. McLerran, R. Venugopalan, Phys. Rev. **D 52**, 2935 (1995).
- [14] A. Ayala, J. Jalilian-Marian, L. McLerran, R. Venugopalan, Phys. Rev. **D 53**, 458 (1996).
- [15] A. Kovner, G. Milhano, Phys. Rev. **D 61**, 014012 (2000).
- [16] A. Kovner, G. Milhano, H. Weigert, Phys. Rev. **D 62**, 114005 (2000).
- [17] E. Iancu, A. Leonidov, L. McLerran, Nucl. Phys. **A 692**, 583 (2001).
- [18] E. Iancu, A. Leonidov, L. McLerran, Phys. Lett. **B 510**, 133 (2001).
- [19] E. Iancu, L. McLerran, Phys. Lett. **B 510**, 145 (2001).
- [20] E. Ferreira, E. Iancu, A. Leonidov, L. McLerran, Nucl. Phys. **A 703**, 489 (2002).
- [21] A. Dumitru, J. Jalilian-Marian, Phys. Rev. Lett. **89**, 022301 (2002).
- [22] A. Dumitru, J. Jalilian-Marian, Phys. Lett. **B 547**, 15 (2002).
- [23] F. Gelis, J. Jalilian-Marian, Phys. Rev. **D 66**, 014021 (2002).
- [24] F. Gelis, J. Jalilian-Marian, hep-ph/0208141, to appear in Phys. Rev. **D**.
- [25] B.Z. Kopeliovich, J. Raufeisen, A.V. Tarasov, Phys. Lett. **B 503**, 91 (2001).
- [26] B.Z. Kopeliovich, J. Raufeisen, A.V. Tarasov, M.B. Johnson, hep-ph/0110221.
- [27] F. Gelis, A. Peshier, Nucl. Phys. **A 697**, 879 (2002).

- [28] F. Gelis, A. Peshier, Nucl. Phys. **A 707**, 175 (2002).
- [29] E. Ferreiro, E. Iancu, K. Itakura, L. McLerran, Nucl. Phys. **A 710**, 373 (2002).
- [30] A.H. Mueller, Nucl. Phys. **B 558**, 285 (1999).
- [31] Yu.V. Kovchegov, Phys. Rev. **D 60**, 034008 (1999).
- [32] K. Golec-Biernat, M. Wusthoff, Phys. Rev. **D 59**, 014017 (1999).
- [33] K. Golec-Biernat, M. Wusthoff, Phys. Rev. **D 60**, 114023 (1999).
- [34] K. Golec-Biernat, M. Wusthoff, Eur. Phys. J. **C 20**, 313 (2001).
- [35] J. Bartels, K. Golec-Biernat, H. Kowalski, Phys. Rev. **D 66**, 014001 (2002).
- [36] A.H. Mueller, Nucl. Phys. **B 335**, 115 (1990).
- [37] K.J. Eskola, V.J. Kolhinen, C.A. Salgado, Eur. Phys. J. **C 9**, 61 (1999).
- [38] S. Peigné, hep-ph/0206138.
- [39] H. Kowalski, private communication.
- [40] F. Gelis, J. Jalilian-Marian, work in progress.